Supplementary Information for Discovery and Quantification of Long-Range RNA Base Pairs in Coronavirus Genomes with SEARCH-MaP and SEISMIC-RNA

Supplementary Figures

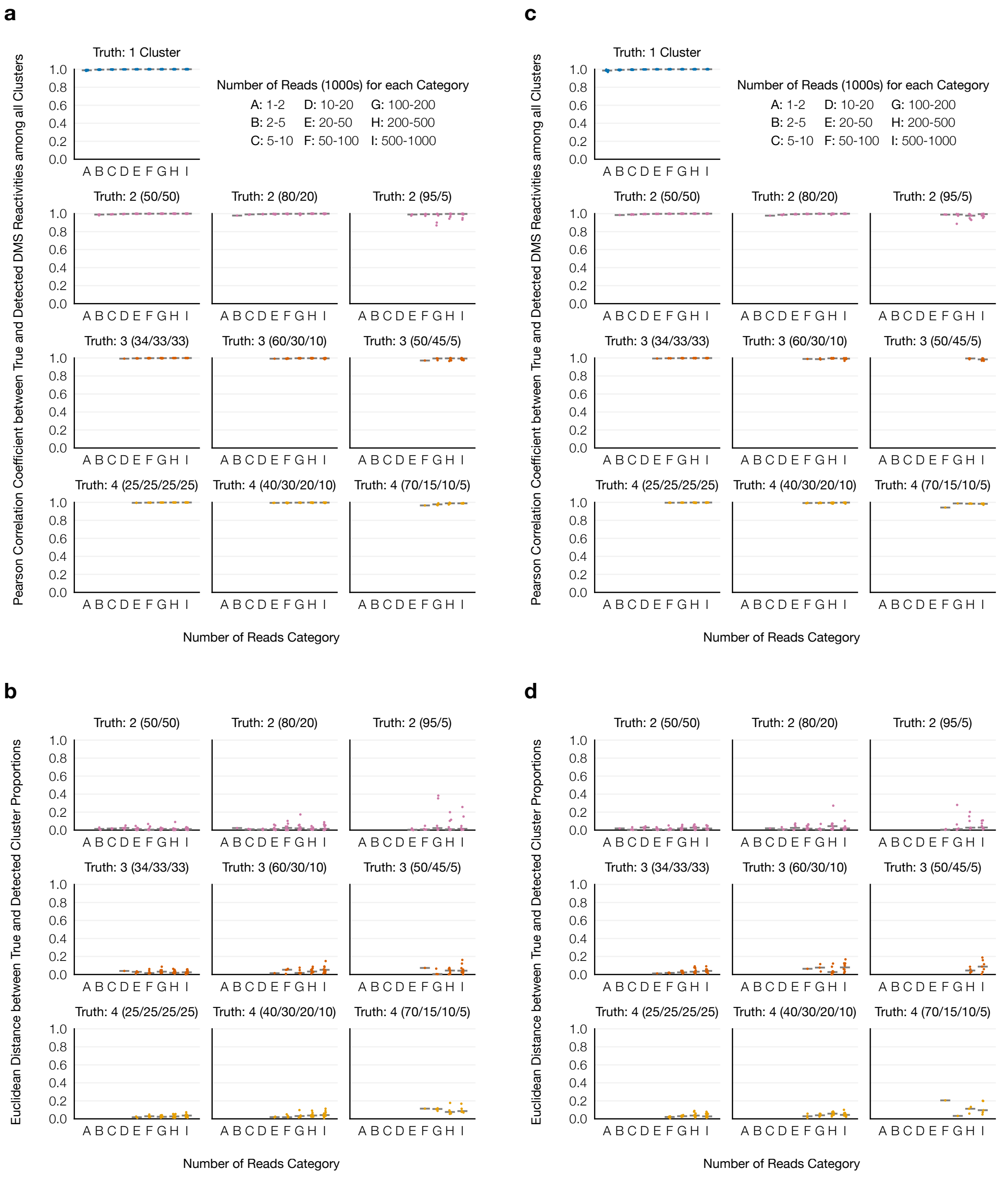

Supplementary Figure 1: **Accuracy of SEISMIC-RNA's clustering algorithm.** Datasets were simulated with one to four "true" alternative structure(s) in three mixing proportions and with 1,000 to 1,000,000 reads (all full-length). For each number of reads, 12 unique 280-nt RNAs were simulated and processed with SEISMIC-RNA. For simulations in which the correct number of clusters was detected, **(a)** the Pearson correlation of the true DMS reactivities versus those calculated by the clustering algorithm and **(b)** the Euclidean distance between the vector of true cluster proportions and those calculated by the clustering algorithm is shown as one point; medians are shown as gray bars. **(c)** and **(d)** Same as (a) and (b), respectively, but reads were simulated with random 5' and 3' ends rather than fully covering the RNA.

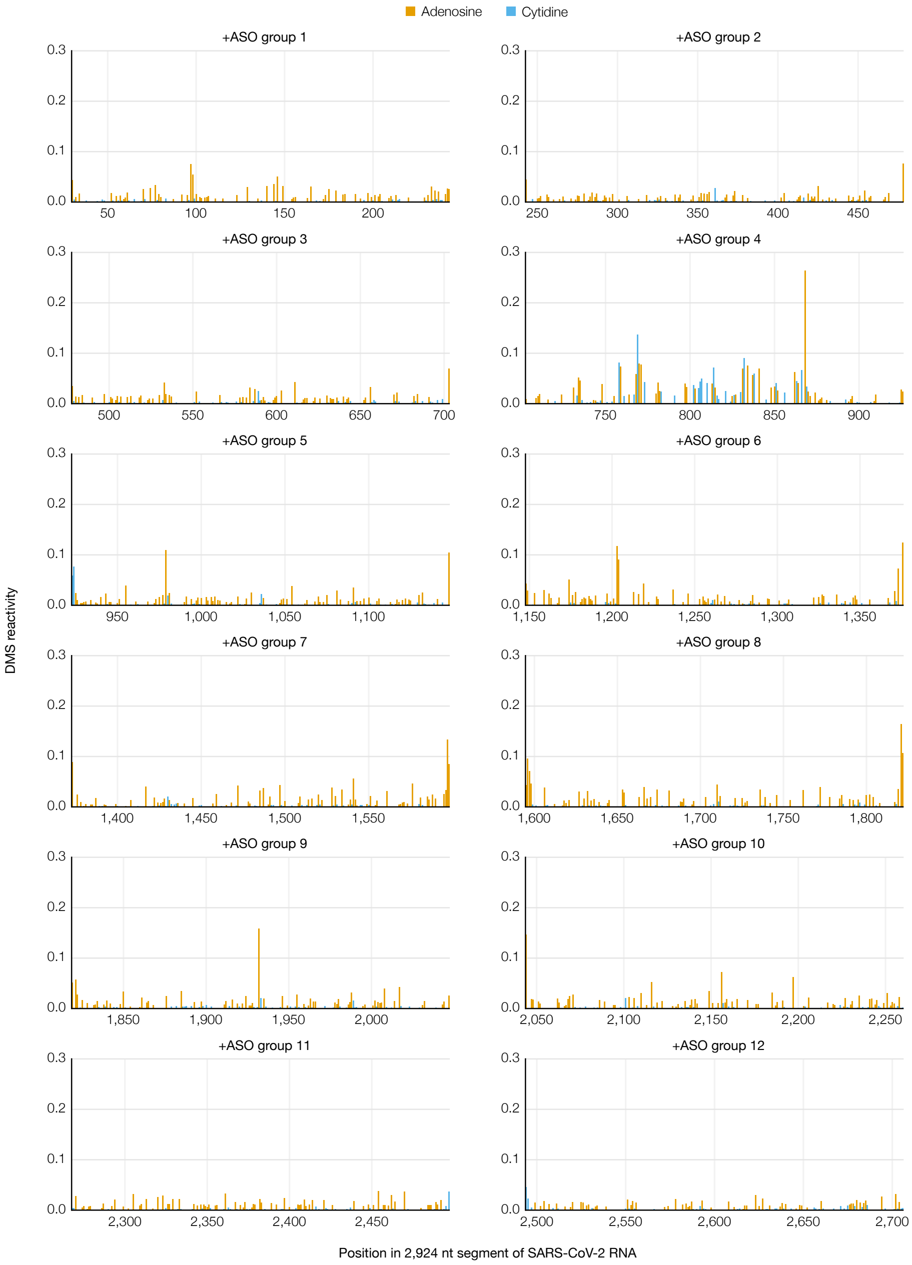

Supplementary Figure 2: **Mutational profile of each ASO target section upon adding the corresponding group of ASOs to the 2,924 nt segment of SARS-CoV-2 genomic RNA.** Positions are colored based on the RNA sequence.

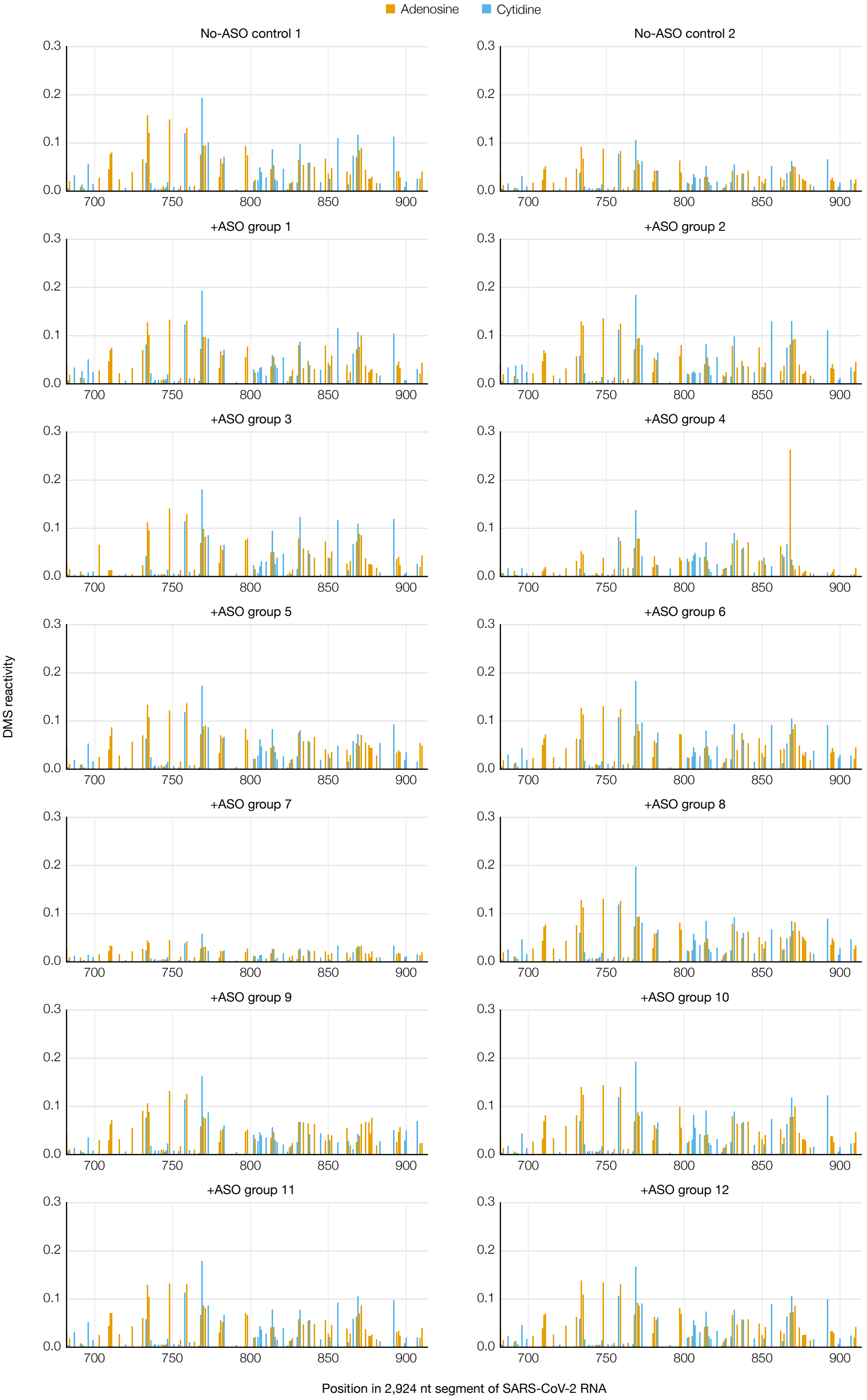

Supplementary Figure 3: **Mutational profiles of the FSE section upon adding each group of ASOs to the 2,924 nt segment of SARS-CoV-2 genomic RNA.** Positions are colored based on the RNA sequence.

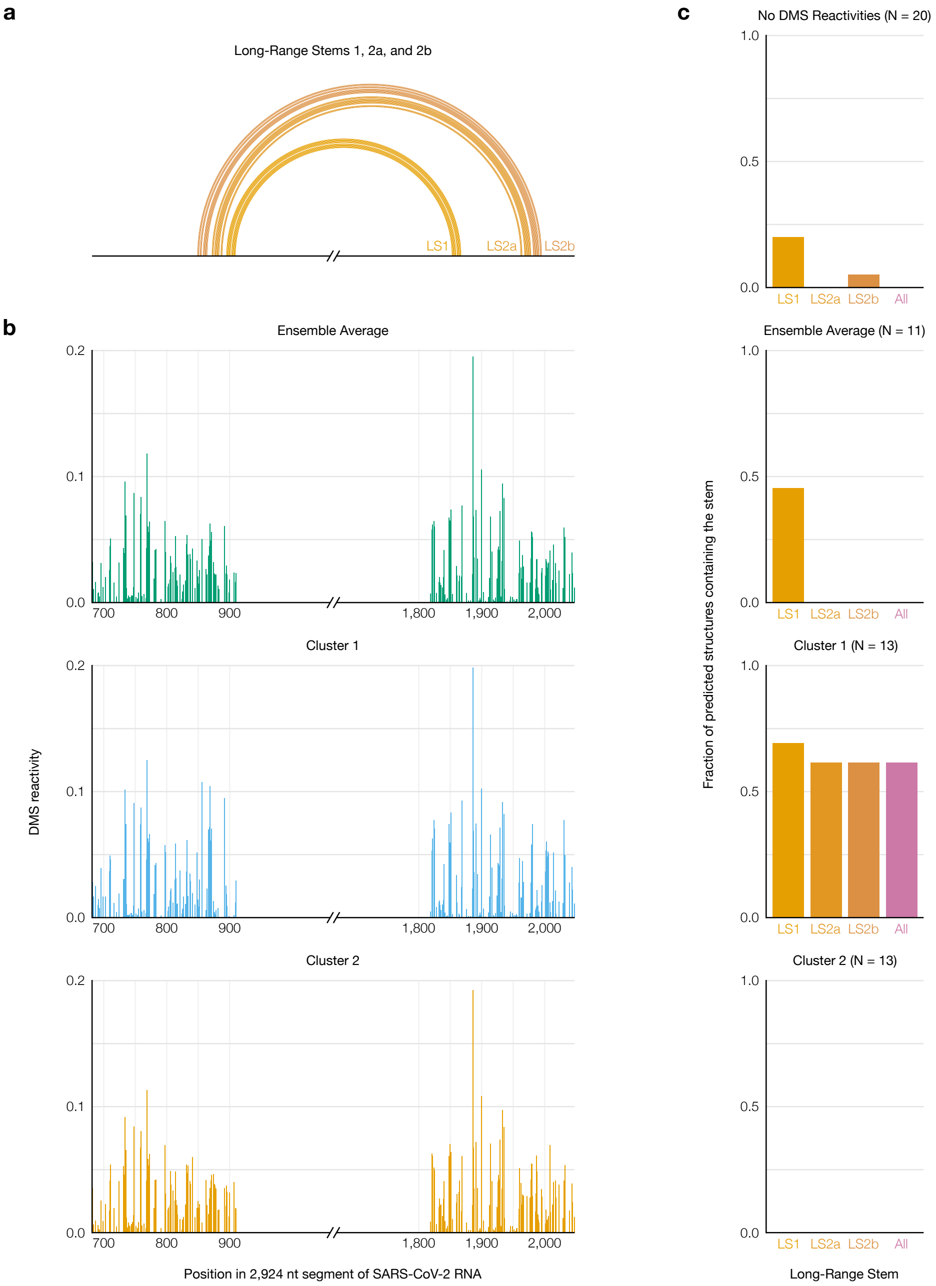

Supplementary Figure 4: **Improved prediction of long-range stems in SARS-CoV-2 using clustered DMS reactivities. (a)** Model of the two inner stems of the FSE-arch [52], denoted long stems (LS) 1 and 2a/b. **(b)** Mutational profiles of the ensemble average and of clusters 1 and 2 on both sides of the FSE-arch. **(c)** For each mutational profile (as well as a purely thermodynamic prediction with no DMS reactivities), the fraction of predicted structures in which each long stem was predicted perfectly (i.e. all base pairs were present). The numbers of predicted structures (N) are indicated.

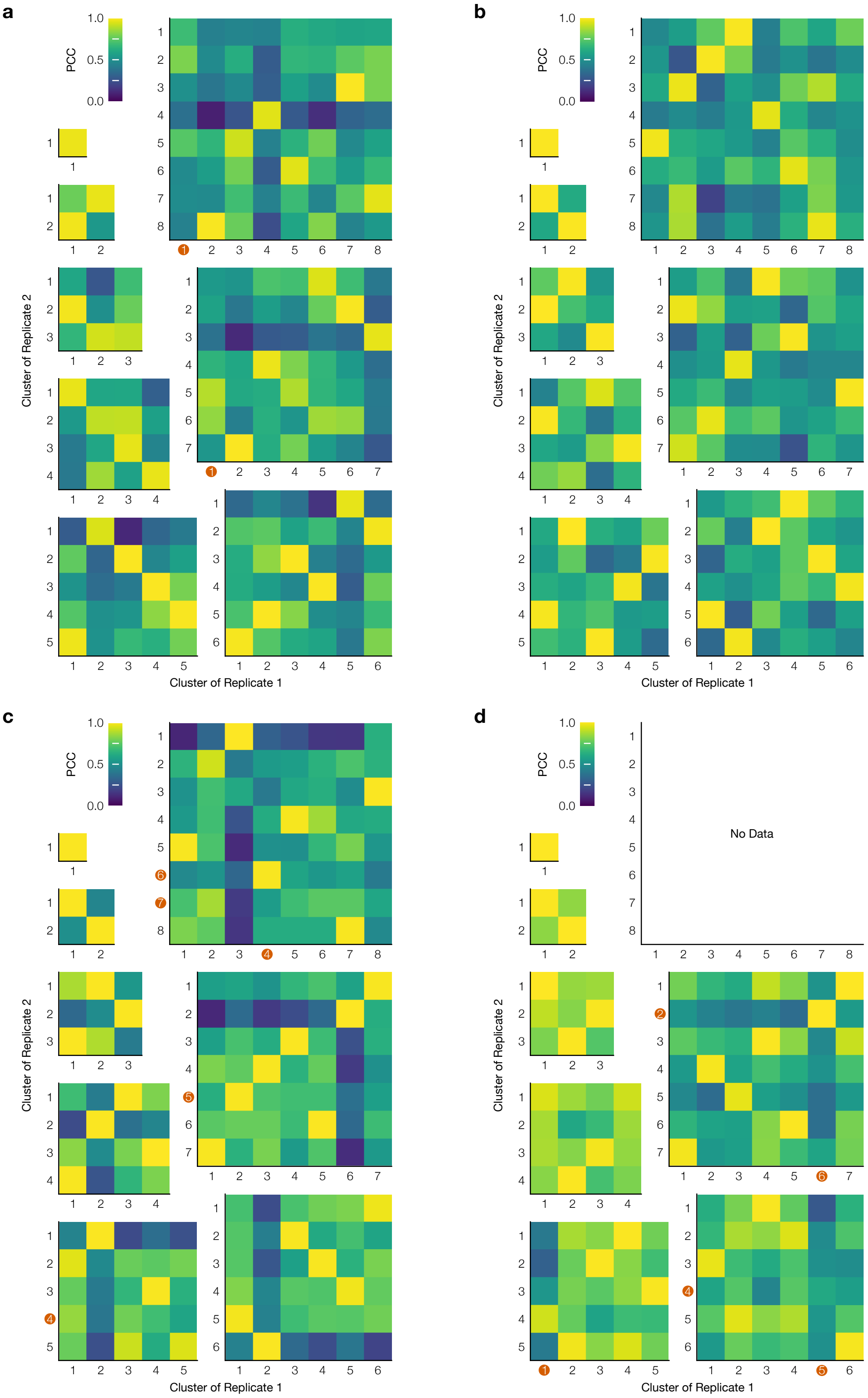

Supplementary Figure 5: **Reproducibility of clustering the SARS-CoV-2 FSE after adding ASOs.** **(a)** Heatmaps of the Pearson correlation coefficient (PCC) between each pair of clusters from two replicates of the 1,799 nt segment of SARS-CoV-2. Each heatmap corresponds to one order (i.e. number of clusters). Clusters are marked with red circles if at least one DMS reactivity exceeded 0.3. **(b)** Same as (a) plus Anti-AS1 ASO. **(c)** Same as (a) plus Anti-PS2-overlap ASO. **(d)** Same as (a) plus Anti-AS1 and Anti-PS2-overlap ASOs.

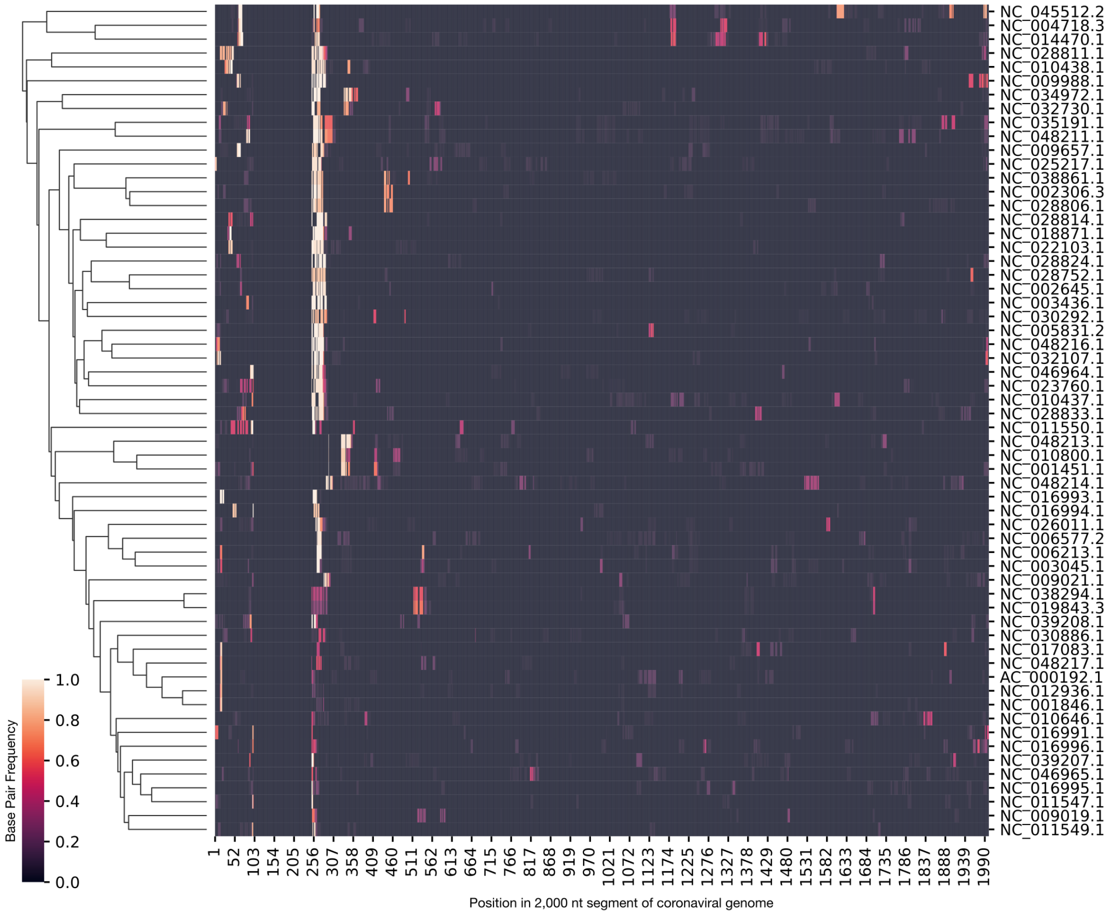

Supplementary Figure 6: **Computational screen of long-range base pairing near the FSE in 60 coronaviruses.** For each 2,000 nt segment of each coronaviral genome, the fraction of predicted structures in which each position outside the range 101-250 base-paired with any position in the range 101-250 is indicated. Genomes are clustered by their base-pairing frequencies. For each genome, the accession number for NCBI [54] is indicated.

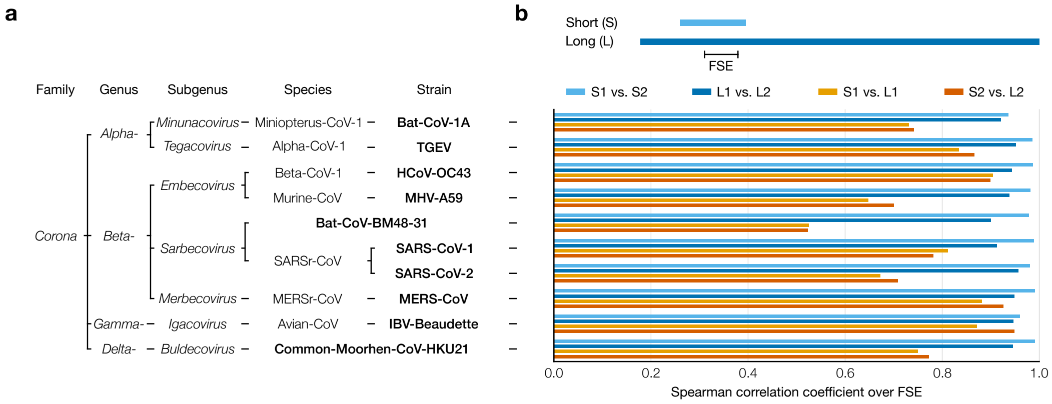

Supplementary Figure 7: **Experimental screen of long-range base pairing near the FSE in 10 coronaviruses. (a)** Taxonomy of the ten coronavirus species/strains in this screen; the lowest-level group for each virus is bolded. Bat-CoV-1A: bat coronavirus 1A (NC_010437.1), TGEV: transmissible gastroenteritis virus (NC_038861.1), HCoV-OC43: human coronavirus OC43 (NC_006213.1), MHV-A59: murine hepatitis virus strain A59 (NC_048217.1), Bat-CoV-BM48-31: bat coronavirus BM48-31 (NC_014470.1), SARS-CoV-1: severe acute respiratory syndrome coronavirus 1 (NC_004718.3), SARS-CoV-2: severe acute respiratory syndrome coronavirus 2 (NC_045512.2), MERS-CoV: Middle East respiratory syndrome coronavirus (NC_019843.3), IBV-Beaudette: avian infectious bronchitis virus strain Beaudette (NC_001451.1), Common-Moorhen-CoV-HKU21: common moorhen coronavirus HKU21 (NC_016996.1). **(b)** Spearman correlation coefficients of DMS reactivities over the FSE between replicates 1 and 2 of short (239 nt) and long (1,799 nt) segments of each coronaviral genome.

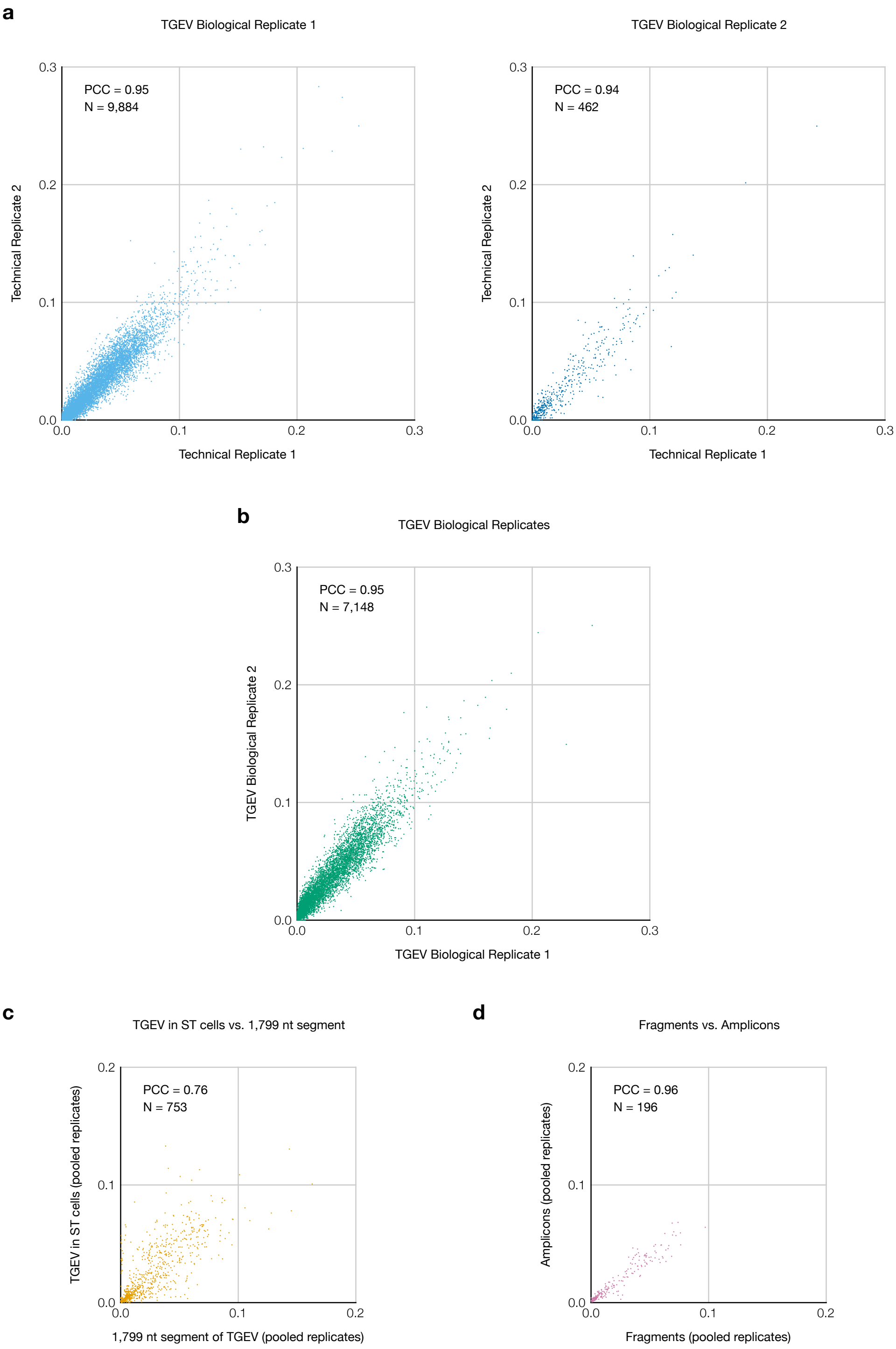

Supplementary Figure 8: **Replicates of TGEV in ST cells and comparison to the 1,799 nt segment.** **(a)** Comparison of DMS reactivities of the two technical replicates for each biological replicate of TGEV in ST cells. Each point represents one base in the sequence. The number of points (N) and Pearson correlation coefficient (PCC) are indicated for each plot. Two bases with DMS reactivities exceeding 0.3 in both technical replicates of biological replicate 1 are not shown. **(b)** Comparison of DMS reactivities of the two biological replicates (pooled technical replicates). One base with DMS reactivity exceeding 0.3 in biological replicate 1 is not shown. **(c)** DMS reactivities of TGEV in ST cells using random fragmentation versus amplicons (pooled biological replicates). **(d)** DMS reactivities of TGEV in ST cells (pooled biological replicates) versus the 1,799 nt segment.

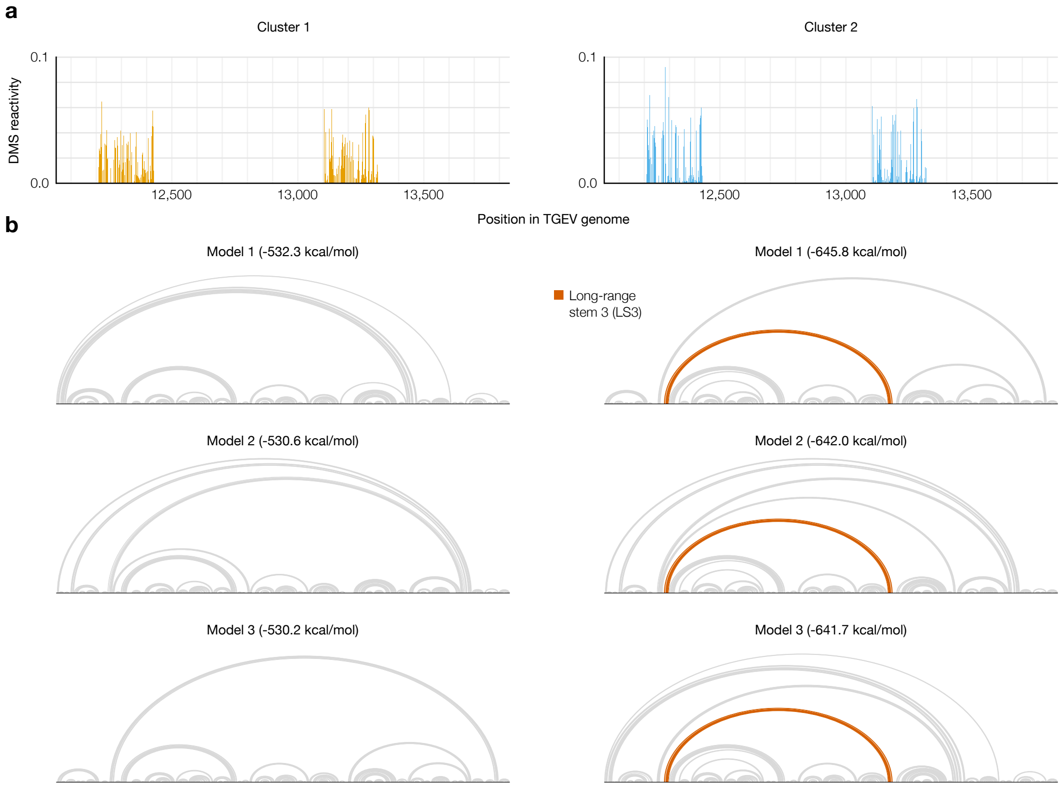

Supplementary Figure 9: **Alternative structures on both sides of the long-range base pairs in TGEV. (a)** DMS reactivities of clusters 1 and 2 on both sides of the long-range base pairs in TGEV, from amplicon samples. **(b)** Three lowest-energy structure models of the 1,799 nt segment (positions 12,042-13,840) based on the DMS reactivities of each cluster. Long-range stem 3 (LS3) is highlighted when it appears in a model. Structures were drawn with VARNA [82].

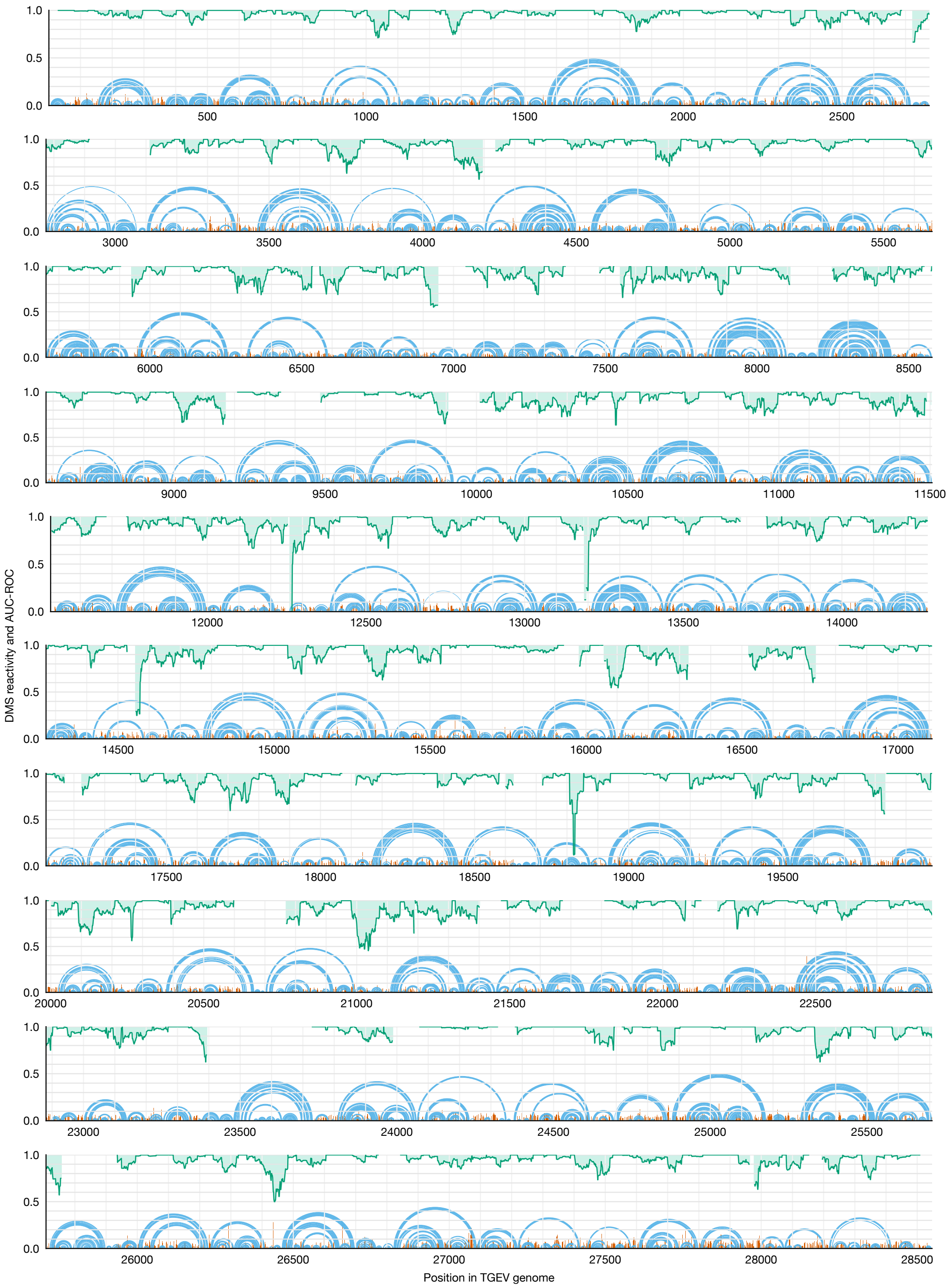

Supplementary Figure 10: **Short-range base pairs across the full TGEV genome.** Model of the secondary structure of the entire TGEV genome with a maximum distance of 300 nt between paired bases (blue). DMS reactivities used to generate the model are shown in red. Rolling (window = 45 nt) area under the receiver operating characteristic curve (AUC-ROC), measuring how well the secondary structure model fits the DMS reactivities, is shown in green.

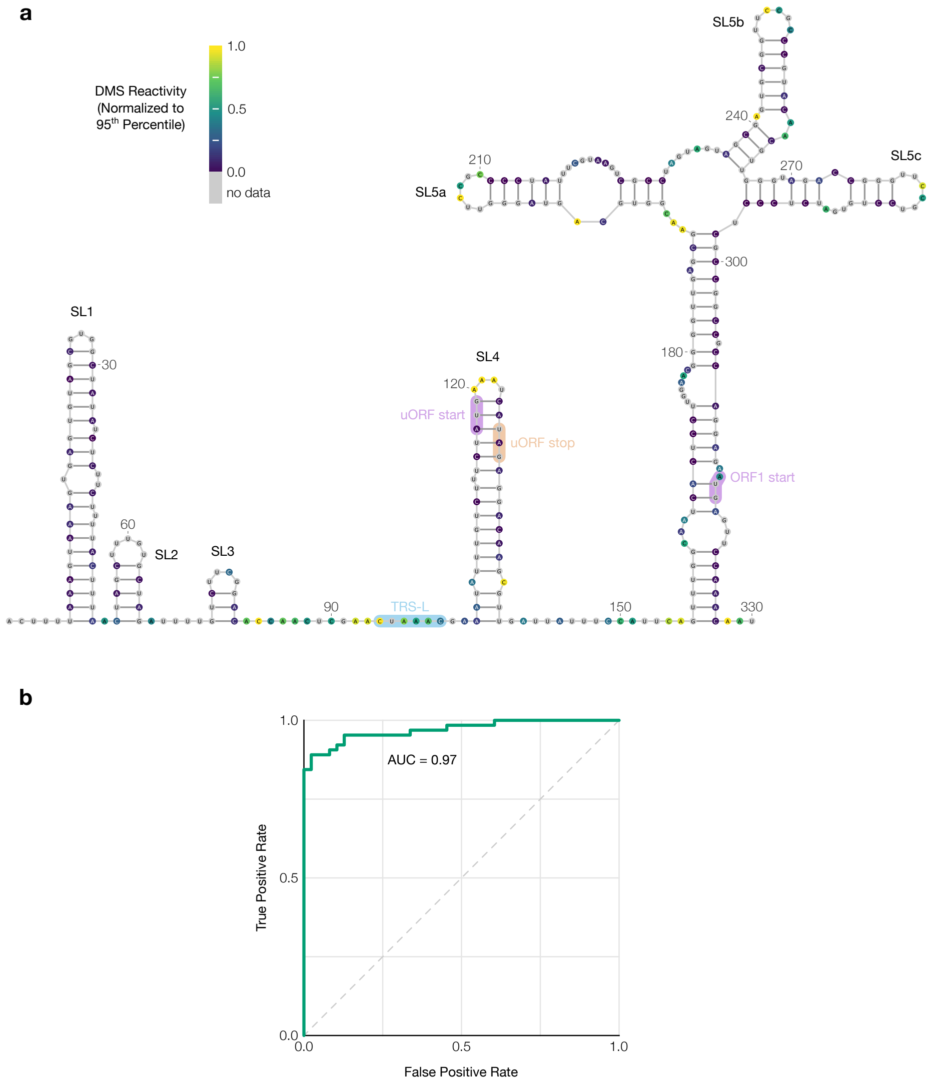

Supplementary Figure 11: **Secondary structure of the TGEV 5' UTR. (a)** Model of the secondary structure of the first 330 nt of the TGEV genome, based on DMS reactivities in infected ST cells normalized to the 95th percentile. Bases are colored by DMS reactivity. The model includes the conserved stem loops SL1, SL2, SL3, SL4, SL5a, SL5b, and SL5c [10]. The leader transcription regulatory sequence (TRS-L) [83], upstream open reading frame (uORF) [84], and start codon of ORF1 are also labeled. The model was drawn using VARNA [82]. **(b)** Receiver operating characteristic curve showing agreement between the DMS reactivities and the secondary structure model; the area under the curve (AUC) is indicated.

Supplementary Methods

Correcting observer bias due to drop-out of reads

Let N reads from K clusters align to a reference sequence of length L. Let the proportion of reads whose 5' and 3' ends align, respectively, to coordinates a and b ($1 \leq a \leq b \leq L$) be η_{ab} (assuming these proportions are equal for all clusters). Let the mutation rate of base j ($1 \leq j \leq L$) in cluster k ($1 \leq k \leq K$) be μ_{jk}. Let the proportion of cluster k in the ensemble be π_k. To express these quantities as probabilities, let C_k be the event that a read comes from cluster k; let E_{ab} be the event that a read aligns with 5' and 3' coordinates a and b, respectively; let S_j be the event that a read contains position j (i.e. its alignment coordinates a and b satisfy $1 \leq a \leq j \leq b \leq L$); let M_j be the event that a read has a mutation at position j; and let G_g be the event that a read has no two mutations separated by fewer than g non-mutated bases.

Deriving mutation rates of reads with no two mutations too close

In terms of these events, the total mutation rates (μ_{jk}) are $P(M_j|S_jC_k)$, i.e. the probability that a read would have a mutation at position j given that it contained position j and came from cluster k; and the observable mutation rates (m_{jk}) are $P(M_j|S_jC_kG_g)$, i.e. the probability that a read would have a mutation at position j given that it contained position j, came from cluster k, and had no two mutations closer than g bases. Using these definitions and Bayes' theorem yields a probabilistic formula for m_{jk}:

$$m_{jk} = P(M_j|S_jC_kG_g) = P(M_j|S_jC_k)\frac{P(G_g|S_jM_jC_k)}{P(G_g|S_jC_k)} = \mu_{jk}\frac{P(G_g|S_jM_jC_k)}{P(G_g|S_jC_k)}$$

The term $P(G_g|S_jC_k)$ is the probability that a read would have no two mutations closer than g bases given that it contained position j and came from cluster k. It can be computed using $P(G_g|E_{ab}C_k)$ (abbreviated d_{abk}): the probability that a read would contain no two mutations closer than g bases given that its 5' and 3' coordinates are a and b, repectively ($1 \leq a \leq b \leq L$), and that it came from cluster k. If position b were mutated (probability μ_{bk}), then the read would contain no two mutations closer than g bases if and only if none of the g bases preceding b (i.e. positions $b-g$ to $b-1$, inclusive) were mutated (probability $\prod_{j'=\text{max}(b-g,a)}^{b-1}(1-\mu_{j'k})$, abbreviated $w_{\text{max}(b-g,a),b-1,k}$) and two no mutations between positions a and $b-(g+1)$, inclusive, were too close (probability $d_{a,\text{max}(b-(g+1),a),k})$). If position b were not mutated (probability $1-\mu_{bk}$), then the read would contain no two mutations closer than g bases if and only if no mutations between positions a and $b-1$, inclusive, were too close (probability $d_{a,\text{max}(b-1,a),k}$). These two possibilities generate a recurrence relation:

$$d_{abk} = \mu_{bk} w_{\text{max}(b-g,a),b-1,k} d_{a,\text{max}(b-(g+1),a),k} + (1-\mu_{bk}) d_{a,\text{max}(b-1,a),k}$$

The base case is $d_{abk} = 1$ when $a = b$ because such a read would contain one position and thus be guaranteed to have no two mutations too close. Then, $P(G_g|S_jC_k)$ is the average of d_{abk} over every read that contains position j, weighted by the proportions η_{ab}:

$$P(G_g|S_jC_k) = \frac{\sum_{a=1}^{j} \sum_{b=j}^{L} \eta_{ab} d_{abk}}{\sum_{a=1}^{j} \sum_{b=j}^{L} \eta_{ab}}$$

The term $P(G_g|S_jM_jC_k)$ is the probability that a read would have no two mutations too close given that it contained a mutation at position j and came from cluster k. It can be computed using $P(G_g|M_jE_{ab}C_k)$ (abbreviated f_{abjk}): the probability that a read would contain no two mutations too close given that position j is mutated ($1 \leq a \leq j \leq b \leq L$), that its 5' and 3' coordinates are a and b (respectively), and that it came from cluster k. Because position j is mutated, having no two mutations too close requires that none of the g bases on both sides of position j be mutated. The probability that none of the preceding g positions ($j-g$ to $j-1$) is mutated is $w_{\text{max}(j-g,a),j-1,k}$, while that of the following g positions ($j+1$ to $j+g$) is $w_{j+1,\text{min}(j+g,b),k}$. Upstream of the g bases flanking position j (i.e. positions a to

$j-(g+1)$), the probability that no two mutations are too close is $d_{a,\mathsf{max}(j-(g+1),a),k}$; downstream (i.e. positions $j+(g+1)$ to b), the probability is $d_{\mathsf{min}(j+(g+1),b),b,k}$. Since mutations in these four sections are independent, the probability that the read contains no two mutations too close is the product:

$$f_{abjk} = d_{a,\mathsf{max}(j-(g+1),a),k} w_{\mathsf{max}(j-g,a),j-1,k} w_{j+1,\mathsf{min}(j+g,b),k} d_{\mathsf{min}(j+(g+1),b),b,k}$$

Then, $P(G_g|S_jM_jC_k)$ is the average of f_{abjk} over every read that contains position j, weighted by the proportions η_{ab}.

$$P(G_g|S_jM_jC_k) = \frac{\sum_{a=1}^{j}\sum_{b=j}^{L}\eta_{ab}f_{abjk}}{\sum_{a=1}^{j}\sum_{b=j}^{L}\eta_{ab}}$$

Combining the above results yields an explicit formula for m_{jk}:

$$m_{jk} = \mu_{jk}\frac{\sum_{a=1}^{j}\sum_{b=j}^{L}\eta_{ab}f_{abjk}}{\sum_{a=1}^{j}\sum_{b=j}^{L}\eta_{ab}d_{abk}}$$

Deriving end coordinate proportions of reads with no two mutations too close

The total proportions (η_{ab}) of reads aligned to 5' and 3' coordinates a and b, respectively, are $P(E_{ab})$; and the proportions of reads with no two mutations too close that align with coordinates a and b (e_{abk}) are $P(E_{ab}|G_gC_k)$. Note that, while reads are assumed to come from the same distribution of coordinates (η_{ab}) regardless of their cluster k, the observable distribution of coordinates (e_{abk}) varies by cluster because P(G_gC_k) depends on k. Using these definitions and Bayes' theorem yields a probabilistic formula for e_{abk}:

$$e_{abk} = P(E_{ab}|G_gC_k) = P(G_g|E_{ab}C_k)\frac{P(E_{ab}|C_k)}{P(G_g|C_k)} = d_{abk}\frac{\eta_{ab}}{P(G_g|C_k)}$$

The term $P(G_g|C_k)$ is the probability that a read would have no two mutations too close given that it came from cluster k. It can be computed as an average of $P(G_g|E_{ab}C_k)$ (i.e. d_{abk}) over all coordinates a and b (such that $1 \leq a \leq b \leq L$), weighted by the proportion of each coordinate, $P(E_{ab})$ (i.e. η_{ab}):

$$P(G_g|C_k) = \frac{\sum_{a=1}^{L}\sum_{b=a}^{L}\eta_{ab}d_{abk}}{\sum_{a=1}^{L}\sum_{b=a}^{L}\eta_{ab}} = \sum_{a=1}^{L}\sum_{b=a}^{L}\eta_{ab}d_{abk}$$

This expression is already normalized because $\sum_{a=1}^{L}\sum_{b=a}^{L}\eta_{ab} = 1$, by definition.

Combining the above results yields an explicit formula for e_{abk}:

$$e_{abk} = \frac{\eta_{ab}d_{abk}}{\sum_{a'=1}^{L}\sum_{b'=a'}^{L}\eta_{a'b'}d_{a'b'k}}$$

Deriving cluster proportions of reads with no two mutations too close

The proportion of total reads in cluster k is $\pi_k = P(C_k)$. The proportion among only reads with no two mutations closer than g bases is

$$p_k = P(C_k|G_g) = P(G_g|C_k)\frac{P(C_k)}{P(G_g)} = \pi_k\frac{\sum_{a=1}^{L}\sum_{b=a}^{L}\eta_{ab}d_{abk}}{P(G_g)}$$

The term $P(G_g)$ is the probability that a read from any cluster would have no two mutations closer than g bases and can be solved for by leveraging that the cluster proportions (p_k) must sum to 1:

$$1 = \sum_{k=1}^{K}p_k = \sum_{k=1}^{K}\pi_k\frac{\sum_{a=1}^{L}\sum_{b=a}^{L}\eta_{ab}d_{abk}}{P(G_g)} = \frac{1}{P(G_g)}\sum_{k=1}^{K}\pi_k\sum_{a=1}^{L}\sum_{b=a}^{L}\eta_{ab}d_{abk}$$

$$P(G_g) = \sum_{k=1}^{K}\pi_k\sum_{a=1}^{L}\sum_{b=a}^{L}\eta_{ab}d_{abk}$$

The result is an explicit formula for p_k:

$$p_k = \frac{\pi_k\sum_{a=1}^{L}\sum_{b=a}^{L}\eta_{ab}d_{abk}}{\sum_{k'=1}^{K}\pi_{k'}\sum_{a=1}^{L}\sum_{b=a}^{L}\eta_{ab}d_{abk'}}$$

Solving total mutation rates and cluster and coordinate proportions

The observed mutation rates (m_{jk}), end coordinate proportions (e_{abk}), and cluster proportions (p_k) can be calculated as weighted averages over the N reads with no two mutations too close:

$$m_{jk} = \frac{\sum_{i=1}^{N} z_{ik} x_{ij}}{\sum_{i=1}^{N} z_{ik} s_{ij}}$$

$$e_{abk} = \frac{\sum_{i=1}^{N} z_{ik} y_{abi}}{\sum_{i=1}^{N} z_{ik}}$$

$$p_k = \frac{\sum_{i=1}^{N} z_{ik}}{N}$$

where s_{ij} is 1 if read i contains position j, otherwise 0; x_{ij} is 1 if read i has a mutation at position j, otherwise 0; y_{abi} is 1 if read i aligns to coordinates a and b, otherwise 0; and z_{ik} is the probability that read i came from cluster k.

The original parameters μ_{jk}, η_{abk}, and π_k can be solved by setting the two formulae each for m_{jk}, e_{abk}, and p_k equal to each other, creating a system of equations:

$$\mu_{jk} \frac{\sum_{a=1}^{j} \sum_{b=j}^{L} \eta_{ab} f_{abjk}}{\sum_{a=1}^{j} \sum_{b=j}^{L} \eta_{ab} d_{abk}} = m_{jk} = \frac{\sum_{i=1}^{N} z_{ik} x_{ij}}{\sum_{i=1}^{N} z_{ik} s_{ij}}$$

$$\eta_{ab} \frac{d_{abk}}{\sum_{a'=1}^{L} \sum_{b'=a'}^{L} \eta_{a'b'} d_{a'b'k}} = e_{ab} = \frac{\sum_{i=1}^{N} z_{ik} y_{abi}}{\sum_{i=1}^{N} z_{ik}}$$

$$\pi_k \frac{\sum_{a=1}^{L} \sum_{b=a}^{L} \eta_{ab} d_{abk}}{\sum_{k'=1}^{K} \pi_{k'} \sum_{a=1}^{L} \sum_{b=a}^{L} \eta_{ab} d_{abk'}} = p_k = \frac{\sum_{i=1}^{N} z_{ik}}{N}$$

Solving this entire system at once has proven computationally impractical for all but extremely short sequences. A more feasible approach is to first solve for μ_{jk} given an initial guess for η_{ab}, next solve for η_{ab} given the updated μ_{jk}, then solve for π_k given the updated μ_{jk} and η_{ab}, and iterate until all three sets of parameters converge.

Even assuming every η_{ab} is a constant, these equations are still too complex to solve for μ_{jk} analytically because d_{abk} and f_{abjk} also depend on μ_{jk} (as well as on other μ variables). Thus, every μ_{jk} is solved for numerically by rearranging each equation to

$$\mu_{jk}\frac{\sum_{a=1}^{j}\sum_{b=j}^{L}\eta_{ab}f_{abjk}}{\sum_{a=1}^{j}\sum_{b=j}^{L}\eta_{ab}d_{abk}} - m_{jk} = 0$$

and applying the Netwon-Krylov method [85] implemented in SciPy [80].

Once every μ_{jk} has been solved for, every η_{ab} can be updated. Because d_{abk} does not depend on η_{ab} (except indirectly through the μ_{jk} parameters, which are now assumed to be constants), each equation can be rearranged to

$$\eta_{ab} = \frac{e_{ab}}{d_{abk}}\sum_{a'=1}^{L}\sum_{b'=a'}^{L}\eta_{a'b'}d_{a'b'k}$$

Leveraging that $\sum_{a=1}^{L}\sum_{b=a}^{L}\eta_{ab} = 1$, by definition, leads to

$$\sum_{a=1}^{L}\sum_{b=a}^{L}\frac{e_{ab}}{d_{abk}}\sum_{a'=1}^{L}\sum_{b'=a'}^{L}\eta_{a'b'}d_{a'b'k} = 1$$

$$\sum_{a'=1}^{L}\sum_{b'=a'}^{L}\eta_{a'b'}d_{a'b'k} = \frac{1}{\sum_{a=1}^{L}\sum_{b=a}^{L}\frac{e_{ab}}{d_{abk}}}$$

and finally a closed-form expression for each η_{ab} given μ_{jk} (and hence d_{abk}) and e_{abk}:

$$\eta_{ab} = \frac{\frac{e_{ab}}{d_{abk}}}{\sum_{a'=1}^{L}\sum_{b'=a'}^{L}\frac{e_{a'b'}}{d_{a'b'k}}}$$

This equation should theoretically yield the same value of η_{ab} for every k. In practice, the values will differ due to inexactness in floating-point arithmetic. Thus, the consensus value of η_{ab} is taken to be the average η_{ab} over every k, weighted by π_k:

$$\eta_{ab} = \sum_{k=1}^{K}\pi_k\frac{\frac{e_{ab}}{d_{abk}}}{\sum_{a'=1}^{L}\sum_{b'=a'}^{L}\frac{e_{a'b'}}{d_{a'b'k}}}$$

With updated values of μ_{jk} and η_{ab}, π_k can also be solved. The above equations can be rearranged to

$$\pi_k = p_k\frac{\sum_{k'=1}^{K}\pi_{k'}\sum_{a=1}^{L}\sum_{b=a}^{L}\eta_{ab}d_{abk'}}{\sum_{a=1}^{L}\sum_{b=a}^{L}\eta_{ab}d_{abk}}$$

Given that $\sum_{k=1}^{K} \pi_k = 1$, by definition:

$$\sum_{k=1}^{K} p_k \frac{\sum_{k'=1}^{K} \pi_{k'} \sum_{a=1}^{L} \sum_{b=a}^{L} \eta_{ab} d_{abk'}}{\sum_{a=1}^{L} \sum_{b=a}^{L} \eta_{ab} d_{abk}} = 1$$

$$\sum_{k'=1}^{K} \pi_{k'} \sum_{a=1}^{L} \sum_{b=a}^{L} \eta_{ab} d_{abk'} = \frac{1}{\sum_{k=1}^{K} \frac{p_k}{\sum_{a=1}^{L} \sum_{b=a}^{L} \eta_{ab} d_{abk}}}$$

which leads to a closed-form expression for each π_k given μ_{jk} (and hence d_{abk}), η_{ab}, and p_k:

$$\pi_k = \frac{\frac{p_k}{\sum_{a=1}^{L} \sum_{b=a}^{L} \eta_{ab} d_{abk}}}{\sum_{k'=1}^{K} \frac{p_{k'}}{\sum_{a=1}^{L} \sum_{b=a}^{L} \eta_{ab} d_{abk'}}}$$

Clustering reads with the expectation-maximization algorithm

Let N reads from K clusters align to a reference sequence of length L. Let the proportion of reads whose 5' and 3' ends align, respectively, to coordinates a and b ($1 \leq a \leq b \leq L$) be η_{ab} (assuming these proportions are equal for all clusters). Let the mutation rate of base j ($1 \leq j \leq L$) in cluster k ($1 \leq k \leq K$) be μ_{jk}. Let the proportion of cluster k in the ensemble be π_k.

Maximization step

The maximization step updates the parameters (μ_{jk}, η_{ab}, and π_k) using the current cluster memberships (z_{ik}). The observed estimates of the parameters m_{jk}, e_{ab}, and p_k are first computed; then, the underlying parameters μ_{jk}, η_{ab}, and π_k are solved for as described in 10.1.4.

Expectation step

The expectation step updates the cluster memberships (z_{ik}) and the likelihood function (L) using the current parameters (μ_{jk}, η_{ab}, and π_k). Each cluster membership is defined as the probability that read i came from cluster k given its

5’/3’ end coordinates (E_{ab}) and mutations (M) and given that no two mutations are too close (G_g): $z_{ik} = P(C_k|E_{ab}MG_g)$. The likelihood of the model (L) is the product of the marginal probability (L_i) of observing each read i from any cluster: $L_i = P(E_{ab}M|G_g)$. Both L_i and z_{ik} can be expressed in terms of the joint probability ($L_{ik} = P(E_{ab}MC_k|G_g)$) of observing each read i from each cluster k:

$$L_i = P(E_{ab}M|G_g) = \sum_{k=1}^{K} P(E_{ab}MC_k|G_g) = \sum_{k=1}^{K} L_{ik}$$

$$z_{ik} = P(C_k|E_{ab}MG_g) = \frac{P(E_{ab}MC_kG_g)}{P(E_{ab}MG_g)} = \frac{P(E_{ab}MC_k|G_g)}{P(E_{ab}M|G_g)} = \frac{L_{ik}}{L_i}$$

To derive a formula for L_{ik}, it can be factored into three parts using the chain rule for probability:

$$L_{ik} = P(E_{ab}MC_k|G_g) = \frac{P(E_{ab}MC_kG_g)}{P(G_g)} = P(M|E_{ab}C_kG_g)P(E_{ab}|C_kG_g)P(C_k|G_g)$$

The first part – the probability that a read would have the specific mutations x_{ij} given that its 5’/3’ end coordinates are a and b (respectively), it comes from cluster k, and no two mutations are too close – is the product over every position j from a to b of the probability of a mutation (μ_{jk}) if read i is mutated at position j ($x_{ij} = 1$), otherwise ($x_{ij} = 0$) the probability of no mutation ($1 - \mu_{jk}$), normalized by the probability that no two mutations would be too close (d_{abk}):

$$P(M|E_{ab}C_kG_g) = \frac{1}{d_{abk}} \prod_{j=a}^{b} \mu_{jk}^{x_{ij}} (1 - \mu_{jk})^{(1-x_{ij})}$$

The second part, $P(E_{ab}|C_kG_g) = e_{abk}$, can be calculated from the parameters μ_{jk}, η_{ab}, and π_k, as explained in 10.1.2. Likewise, the third part, $P(C_k|G_g) = p_k$, can also be calculated from the parameters, as explained in 10.1.3. Combining all parts yields a formula for L_{ik} in terms of the parameters μ_{jk}, η_{ab}, and π_k and of their derived values d_{abk}, e_{abk}, and p_k:

$$L_{ik} = p_k \frac{e_{abk}}{d_{abk}} \prod_{j=a}^{b} \mu_{jk}^{x_{ij}} (1 - \mu_{jk})^{(1-x_{ij})}$$

The formula for the total likelihood of the model and its parameters follows:

$$L(\mu, \eta, \pi) = \prod_{i=1}^{N} L_i = \prod_{i=1}^{N} \sum_{k=1}^{K} p_k \frac{e_{abk}}{d_{abk}} \prod_{j=a}^{b} \mu_{jk}^{x_{ij}} (1 - \mu_{jk})^{(1-x_{ij})}$$

Supplementary Tables

Table 1: **Sequences of the antisense oligonucleotides (ASOs) targeting the 2,924 nt segment of SARS-CoV-2 RNA.**

Group	ASO	Sequence
1	1	GGCAGCACAAGACATCTGTCGTAGTGCAACAGGACTAAGCTCATTATT
	2	TGTAGTAAGCTAACGCATTGTCATCAGTGCAAGCAGTTTGTGTAGTACC
	3	TGTAAATCGGATAACAGTGCAAGTACAAACCTACCTCCCTTTGTTGTGT
	4	GATAGTACCAGTTCCATCACTCTTAGGGAATCTAGCCCATTTCAAATCC
	5	CTTTAGGTGTGTCTGTAACAAACCTACAAGGTGGTTCCAGTTCTGTATA
2	1	ATACCTCTATTTAGGTTGTTTAATCCTTTAATAAAGTATAAATACTTCACTTTAGGAC
	2	CACTTCTGTTGCATTACCAGCTTGTAGACGTACTGTGGCAGCTAAACTACCAAGTACC
	3	AAGCTTTAGCAGCATCTACAGCAAAAGCACAGAAAGATAATACAGTTGAATTGGCAGG
	4	CACAACATCTTAACACAATTAGTGATTGGTTGTCCCCCACTAGCTAGATAATCTTTGT
3	1	GATCCATATTGGCTTCCGGTGTAACTGTTATTGCCTGACCAGTACCAGTGTGTGTA
	2	ATGATCTATGTGGCAACGGCAGTACAGACAACACGATGCACCACCAAAGGATTCTT

Continued on next page

Table 1: **Sequences of the antisense oligonucleotides (ASOs) targeting the 2,924 nt segment of SARS-CoV-2 RNA.** (Continued)

	3	GTTGTAGGTATTTGTACATACTTACCTTTTAAGTCACAAAATCCTTTAGGATTTGG
	4	CCGCAGACGGTACAGACTGTGTTTTTAAGTGTAAAACCCACAGGGTCATTAGCACAA
4	1	CTGAAGCATGGGTTCGCGGAGTTGATCACAACTACAGCCATAACCTTTCCACATA
	2	GGAAGCGACAACAATTAGTTTTTAGGAATTTAGCAAAACCAGCTACTTTATCATTG
5	1	TGTCTCTTAACTACAAAGTAAGAATCAATTAAATTGTCATCTTCGTCCTTTTCTT
	2	GACAATCCTTAAGTAAATTATAAATTGTTTCTTCATGTTGGTAGTTAGAGAAAGTG
	3	GGTACCATGTCACCGTCTATTCTAAACTTAAAGAAGTCATGTTTAGCAACAGCTG
	4	AAGCATAGACGAGGTCTGCCATTGTGTATTTAGTAAGACGTTGACGTGATATATGT
6	1	TGTATGTGACAAGTATTTCTTTTAATGTGTCACAATTACCTTCATCAAAATGCCTTA
	2	GGTTTTCTACAAAATCATACCAGTCCTTTTTATTGAAATAATCATCATCACAACAAT
	3	TTAACAAAGCTTGGCGTACACGTTCACCTAAGTTGGCGTATACGCGTAATATATCTG
	4	ATGTCAGTACACCAACAATACCAGCATTTCGCATGGCATCACAGAATTGTACTGTTT

Continued on next page

Table 1: **Sequences of the antisense oligonucleotides (ASOs) targeting the 2,924 nt segment of SARS-CoV-2 RNA.** (Continued)

7	1	GTTTGTATGAAATCACCGAAATCATACCAGTTACCATTGAGATCTTGATTATCTA
	2	TAGGCATTAACAATGAATAATAAGAATCTACAACAGGAACTCCACTACCTGGCGTG
	3	GTTAAGTCAGTGTCAACATGTGACTCTGCAGTTAAAGCCCTGGTCAAGGTTAATA
	4	TTAACCTCTCTTCCGTGAAGTCATATTTTAACAAATCCCACTTAATGTAAGGCTTT
8	1	AACACAATTTGGGTGGTATGTCTGATCCCAATATTTAAAATAACGGTCAAAGAGTT
	2	GAGAATAAAACATTAAAGTTTGCACAATGCAGAATGCATCTGTCATCCAAACAGTT
	3	CATCAACAAATATTTTTCTCACTAGTGGTCCAAAACTTGTAGGTGGGAACACTGTA
	4	ATGTACAACACCTAGCTCTCTGAAGTGGTATCCAGTTGAAACTACAAATGGAACAC
9	1	TACACAAGTAATTCCTTAAAACTAAGTCTAGAGCTATGTAAGTTTACATCCTGATT
	2	TGCGTTTATCTAGTAATAGATTACCAGAAGCAGCGTGCATAGCAGGGTCAGCAGCA
	3	TTTGACAGTTTGAAAAGCAACATTGTTAGTAAGTGCAGCTACTGAAAAGCACGTAG
	4	CTTAAAGAAACCCTTAGACACAGCAAAGTCATAGAAGTCTTTGTTAAAATTACCGGG

Continued on next page

Table 1: **Sequences of the antisense oligonucleotides (ASOs) targeting the 2,924 nt segment of SARS-CoV-2 RNA.** (Continued)

10	1	CAGCATTACCATCCTGAGCAAAGAAGAAGTGTTTTAATTCAACAGAACTTCCTTC
	2	CTGATATCACACATTGTTGGTAGATTATAACGATAGTAGTCATAATCGCTGATAG
	3	ACCATCGTAACAATCAAAGTACTTATCAACAACTTCAACTACAAATAGTAGTTGT
	4	AACCAGCTGATTTGTCTAGGTTGTTGACGATGACTTGGTTAGCATTAATACAGCC
11	1	CCTCATAACTCATTGAATCATAATAAAGTCTAGCCTTACCCCATTTATTAAATGGAA
	2	ATTTGAGTTATAGTAGGGATGACATTACGTTTTGTATATGCGAAAAGTGCATCTTGAT
	3	GAGACACCAGCTACGGTGCGAGCTCTATTCTTTGCACTAATGGCATACTTAAGATTC
	4	GGCTATTGATTTCAATAATTTTTGATGAAACTGTCTATTGGTCATAGTACTACAGATA
12	1	CAACCACCATAGAATTTGCTTGTTCCAATTACTACAGTAGCTCCTCTAGTGGC
	2	CCATAAGGTGAGGGTTTTCTACATCACTATAAACAGTTTTTAACATGTTGTGC
	3	CATAATTCTAAGCATGTTAGGCATGGCTCTATCACATTTAGGATAATCCCAAC
	4	ACGGTGTGACAAGCTACAACACGTTGTATGTTTGCGAGCAAGAACAAGTGAGGC

Continued on next page

Table 1: **Sequences of the antisense oligonucleotides (ASOs) targeting the 2,924 nt segment of SARS-CoV-2 RNA.** (Continued)

13	1	ACACATGACCATTTCACTCAATACTTGAGCACACTCATTAGCTAATCTATAGAA
	2	AGTTGTGGCATCTCCTGATGAGGTTCCACCTGGTTTAACATATAGTGAACCGCC
	3	ATTAACATTGGCCGTGACAGCTTGACAAATGTTAAAAACACTATTAGCATAAGC
	4	TAAATTGCGGACATACTTATCGGCAATTTTGTTACCATCAGTAGATAAAAGTGC

Table 2: **Sequences of the forward (F) and reverse (R) primers for amplifying the target site of each ASO group in the 2,924 nt segment of SARS-CoV-2 RNA.**

Group	Primer	Sequence
1	F	AATAATGAGCTTAGTCCTGTTGCACTACG
	R	AGGTTGTTTAATCCTTTAATAAAGTATAAATACTTCACTTTAGG
2	F	ACCTTGTAGGTTTGTTACAGACACACCTAA
	R	TTGCCTGACCAGTACCAGTGTGTG
3	F	GGACAACCAATCACTAATTGTGTTAAGATGTTG
	R	TCACAACTACAGCCATAACCTTTCCACA
4	F	CTTAAAAACACAGTCTGTACCGTCTGC
	R	GTAAGAATCAATTAAATTGTCATCTTCGTCCTTTTC
5	F	TGCTAAATTCCTAAAAACTAATTGTTGTCGCTT
	R	ATGTGTCACAATTACCTTCATCAAAATGCCT
6	F	CAATGGCAGACCTCGTCTATGC
	R	GAAATCATACCAGTTACCATTGAGATCTTGATTATC
7	F	CGAAATGCTGGTATTGTTGGTGTACTGAC
	R	GTCTGATCCCAATATTTAAAATAACGGTCAAAGAG
8	F	TGTTAAAATATGACTTCACGGAAGAGAGGTT
	R	AAGTCTAGAGCTATGTAAGTTTACATCCTGA
9	F	CCACTTCAGAGAGCTAGGTGTTGTAC
	R	CAAAGAAGAAGTGTTTTAATTCAACAGAACTTCCT
10	F	TGACTTTGCTGTGTCTAAGGGTTTCTTTA
	R	CATAATAAAGTCTAGCCTTACCCCATTTATTAAATGG
11	F	CGTCAACAACCTAGACAAATCAGCTGG

Continued on next page

Table 2: **Sequences of the forward (F) and reverse (R) primers for amplifying the target site of each ASO group in the 2,924 nt segment of SARS-CoV-2 RNA.** (Continued)

	R	TTCCAATTACTACAGTAGCTCCTCTAGTG
12	F	GACCAATAGACAGTTTCATCAAAAATTATTGAAATCAATAG
	R	ATACTTGAGCACACTCATTAGCTAATCTATAG
13	F	ACAACGTGTTGTAGCTTGTCACACC
	R	TAAATTGCGGACATACTTATCGGCAATTTTG

Table 3: **Sequences of the antisense oligonucleotides (ASOs) targeting the 1,799 nt segment of SARS-CoV-2 genomic RNA.** A plus sign (+) indicates that the following nucleotide is locked nucleic acid (LNA).

ASO	Sequence
Anti-LS1	GTAATTC+CTTAAAA+CTAAG
Anti-LS2a	TGAAA+AGCAA+CATTGTT
Anti-LS2b	TA+CCGGGTTTGACAG
Anti-LS3b	A+CCCTTAGACACAGCA
Anti-AS1	TGGGTTCGCG+GAGTTG
Anti-PS2-overlap	GT+TAAAATTA+CCG+GG

Table 4: **PCR primer annealing temperatures for coronavirus gene fragments.**

Coronavirus	**Annealing Temperature (°C)**
Bat Coronavirus 1A	55
Bat Coronavirus BM48-31	60
Common Moorhen Coronavirus	55
Human Coronavirus OC43	55
Infectious Bronchitis Virus	60
MERS Coronavirus	60
Murine Hepaitis Virus	60
SARS Coronavirus 1	60
SARS Coronavirus 2	55
Transmissible Gastroenteritis Virus	55

Table 5: **Sequences of the forward (F), forward with T7 promoter (F+T7), and reverse (R) primers for amplifying the 239 nt segment of each 1,799 nt segment of coronaviral RNAs.**

Coronavirus	Primer	Sequence
Bat Coronavirus 1A	F	GGACCCTATACGGTTTTGT-CTTGAAAA
	F+T7	TAATACGACTCACTATAGGA-CCCTATACGGTTTTGTCTTG-AAAA
	R	TTTTACAATAAAGAAAGCAT-CATGCTT
Bat Coronavirus BM48-31	F	GGGTTTTATTCTTAGAAACA-CAGTCTG
	F+T7	TAATACGACTCACTATAGG-GTTTTATTCTTAGAAACACA-GTCTG
	R	GGAGTCTAATAAGTTGCCC-TCTTCATC
Common Moorhen Coronavirus	F	GGATAAAGATAAGGAACCT-GTTTCTTT
	F+T7	TAATACGACTCACTATAGGA-TAAAGATAAGGAACCTGTTT-CTTT
	R	ACTATTAGGTATTGGCAAAT-TAATGCG
Human Coronavirus OC43	F	GGCTGTGTCTTATGTTTTGA-CACATGA

Continued on next page

Table 5: **Sequences of the forward (F), forward with T7 promoter (F+T7), and reverse (R) primers for amplifying the 239 nt segment of each 1,799 nt segment of coronaviral RNAs.** (Continued)

	F+T7	TAATACGACTCACTATAGGCTGTGTCTTATGTTTTGACACATGA
	R	ATCTAATTTATCACCGTTCTCATCAAC
Infectious Bronchitis Virus	F	GGTTTGCACTGTTTGCCAGTGTTGGAT
	F+T7	TAATACGACTCACTATAGGTTTGCACTGTTTGCCAGTGTTGGAT
	R	CTCAAGATTTCCATCTTCAGTATCGCG
MERS Coronavirus	F	GGGATTTTGTTTGTCAAATACCCCCTG
	F+T7	TAATACGACTCACTATAGGGATTTTGTTTGTCAAATACCCCCTG
	R	ATGATGCCCTTGGTCATCTAATTCTAC
Murine Hepatitis Virus	F	GGCTGTGTCATATGTGTTGACGCATGA
	F+T7	TAATACGACTCACTATAGGCTGTGTCATATGTGTTGACGCATGA

Continued on next page

Table 5: **Sequences of the forward (F), forward with T7 promoter (F+T7), and reverse (R) primers for amplifying the 239 nt segment of each 1,799 nt segment of coronaviral RNAs.** (Continued)

	R	ATCCAACTTGTTGCCGTCCTCATCTAC
SARS Coronavirus 1	F	GGGTTTTACACTTAGAAACACAGTCTG
	F+T7	TAATACGACTCACTATAGGGTTTTACACTTAGAAACACAGTCTG
	R	AGAGTCTAATAAATTGCCTTCCTCATC
SARS Coronavirus 2	F	GGGTTTTACACTTAAAAACACAGTCTG
	F+T7	TAATACGACTCACTATAGGGTTTTACACTTAAAAACACAGTCTG
	R	AGAATCAATTAAATTGTCATCTTCGTC
Transmissible Gastroenteritis Virus	F	GGCAATTCGGTTCTGTATTGAAAATGA
	F+T7	TAATACGACTCACTATAGGCAATTCGGTTCTGTATTGAAAATGA
	R	TTTGACAATGTAGTAGGCATCATGTTT

Table 6: **Sequences of the antisense oligonucleotides (ASOs) targeting the 1,799 nt segments of coronaviral RNAs.**

Coronavirus	ASO	Sequence
Bat Coronavirus 1A	1	CAGGGCTCTAGTCGAGCTGCACTAGAGCCCCTTGCTCGTTTAAATAAGCCTGATCAACAG
	2	GCAACTTCTTTATTGTAAATATCAAAGGCGCGTACAACATGCTCCGGTTCAGTACCATTA
Bat Coronavirus BM48-31	1	GACATCAGTGCTTGTGCCTGTGCCGCACGGTGTAAGACGGGCCGCACTTACACCGCAAAC
	2	TTTTAGGAACTTTGCAAAACCAGCAACTTTCTCATTATAAATATCAAAAGCCCTGTAAAC
	3	AAAATAGGAGTCTAATAAGTTGCCCTCTTCATCAACTTCCTGGAAACGGCAACAATTTGT
Common Moorhen Coronavirus	1	TGGGGTTCTAGACGGGCATCACTAGAACCCTTTACTCGTTTAAATAAGCTGTATTTTGCA
	2	GTTATATTATTATGTACATGAAACGCCCTTTTTACAATATCCGGCTGAGTGCCAGACTGT
Infectious Bronchitis Virus	1	ACATCAAAGGCTCGCTTTACAACATCAGGATCACATCCACTAGCAAGGGGTATCAGCCGA

Continued on next page

Table 6: **Sequences of the antisense oligonucleotides (ASOs) targeting the 1,799 nt segments of coronaviral RNAs.** (Continued)

Murine Hepatitis Virus	1	AAGCCACTGGCACAGGGTACAAGACGGGCATTTACACTTGTACCCCGAATCCGTTTAAAA
	2	CCAATGCCAGCTCGATTAGCATTACAAATGTCAAATGCCCTTAATTGAACATCAGTGTCC
	3	AACTTGTTGCCGTCCTCATCTACACGCTGGAAGCGGCAGCAATTCACTTTATAATACAAA
SARS Coronavirus 1	1	TTTGCAAAACCAGCAACTTTTTCGTTGTAAATATCAAAAGCCCTGTAGACGACATCAGTA
	2	TCTAATAAATTGCCTTCCTCATCCTTCTCCTGGAAGCGACAGCAATTAGTTTTTAGGAAC
SARS Coronavirus 2	1	GACATCAGTACTAGTGCCTGTGCCGCACGGTGTAAGACGGGCTGCACTTACACCGCAAAC
	2	TTTTAGGAATTTAGCAAAACCAGCTACTTTATCATTGTAGATGTCAAAAGCCCTGTATAC
Transmissible Gastroenteritis Virus	1	TAAATAACTTTGATCAACAGTAAAACTCTGCATAGAAGTACGATCGCACATGCAACCATT

Continued on next page

Table 6: **Sequences of the antisense oligonucleotides (ASOs) targeting the 1,799 nt segments of coronaviral RNAs.** (Continued)

2	GGTCTGGATCAGTACCATTGC-AGGGTTCTAGTCGAGCTGCA-CTAGAACCCCGCACTCGTT